Influence of an internally–generated QBO on modeled stratospheric dynamics and ozone

M. M. Hurwitz [1, 2, 3], **P. A. Newman** [3] and **I.–S. Song** [3, 4, *]

1 *NASA Postdoctoral Program, NASA Goddard Space Flight Center, Greenbelt, MD, USA*

2 *Goddard Earth Science Technology and Research (GESTAR), Morgan State University, Baltimore, MD, USA*

3 *NASA Goddard Space Flight Center, Greenbelt, MD, USA*

4 *Goddard Earth Sciences and Technology Center (GEST), University of Maryland, Baltimore County, Baltimore, MD, USA*

* *Now at: Next Generation Model Development Project, Korea Meteorological Administration, Seoul, South Korea*

Abstract

A GEOS V2 CCM simulation with an internally generated quasi–biennial oscillation (QBO) signal is compared to an otherwise identical simulation without a QBO. In a present–day climate, inclusion of the modeled QBO makes a significant difference to stratospheric dynamics and ozone throughout the year. The QBO enhances variability in the tropics, as expected, but also in the polar stratosphere in some seasons. The modeled QBO also affects the mean stratospheric climate. Because tropical zonal winds in the baseline simulation are generally easterly, there is a relative increase in zonal wind magnitudes in tropical lower and middle

stratosphere in the QBO simulation. Extra–tropical differences between the QBO and 'no QBO' simulations thus reflect a bias toward the westerly phase of the QBO: a relative strengthening and poleward shifting the polar stratospheric jets, and a reduction in Arctic lower stratospheric ozone.

1 Introduction

The quasi–biennial oscillation (QBO) is the leading mode of variability in the tropical lower and middle stratosphere [Baldwin et al., 2001]. The QBO is characterized by a downward–propagating pattern of alternating easterly and westerly zonal winds in the equatorial region, with a period of 28 months (Figure 1a), and is driven by gravity and planetary–scale waves. The zonal wind QBO induces changes in the tropical stratospheric circulation, affecting the concentrations of ozone and other trace constituents [Gray et al., 1989; Butchart et al., 2003; Tian et al., 2006].

The phase of the QBO affects the polar stratosphere. Holton and Tan [1980] and Lu et al. [2008] showed that the phase of the QBO modulates the strength of the Arctic vortex in mid–winter; the vortex is weakest during the easterly phase of the QBO. Hurwitz et al. [2011a, 2011b] found that the phase of the QBO modulates the strength of the Antarctic vortex in austral summer, during warm pool El Niño (WPEN) events [see Kug et al., 2009]. Analogously to the Arctic response, the Antarctic vortex is weakest during WPEN events coincident with the easterly phase of the QBO. In addition, QBO phase–related differences in the strength of the polar vortices modulate polar ozone loss [Lait, 1989; Randel and Cobb, 1994]. However, as the QBO signal is intrinsic to the observational record, the time–averaged impact of the easterly and westerly phases of the QBO on mean zonal wind, temperature and ozone cannot be evaluated using atmospheric data.

A chemistry-climate model (CCM) is the ideal tool for understanding the net impact of the QBO. Punge and Giorgetta [2008] quantified the net effect of the QBO on the late 20th century stratospheric climate by comparing two CCM simulations: one without a QBO signal, and the other with zonal winds between 90 hPa and 10 hPa nudged to profiles taken at Singapore. The authors found that inclusion of the QBO signal made a significant difference to zonal winds, temperature and ozone, mainly in the deep tropics. The vertical pattern of changes in tropical upwelling was consistent with changes in the transport of trace species. However, the value of the conclusions reached by Punge and Giorgetta [2008] is limited because the authors tested a prescribed QBO. Nudging to observed zonal winds does not allow the tropical and mid–latitude stratosphere to adjust realistically to changes in e.g., the QBO phase, nor does it allow for full interaction between stratospheric ozone and climate.

The Goddard Earth Observing System Chemistry–Climate Model, Version 2 (GEOS V2 CCM) can be run with or without an internally–generated QBO. In the formulation of the GEOS V2 CCM evaluated by SPARC CCMVal [2010], both tropical lower stratospheric variability and the QBO amplitude were negligible, typical of CCMs that lack a nudged or internal QBO signal. In contrast, a more recent model formulation [introduced by Hurwitz et al., 2011b] has an internally–generated QBO with a realistic periodicity and amplitude. Comparing the two formulations of the GEOS V2 CCM, this paper quantifies the net effect of an internally generated QBO on stratospheric climate and variability. Section 2 provides a brief description of the two formulations of the CCM, as well as the simulations used to test the net impact of an internal QBO on the stratosphere. The effects of the internal QBO on the mean and variance of zonal winds, temperature and ozone are shown in Section 3. Section 4 provides a summary and discussion of the implication of the results for future CCM studies.

2 Model and simulations

This paper considers the net impact of the QBO in the GEOS V2 CCM. The GEOS V2 CCM couples the GEOS–5 general circulation model (GCM) [Molod et al., 2011] with a comprehensive stratospheric chemistry module [Pawson et al., 2008]. The model has 2° latitude × 2.5° longitude horizontal resolution and 72 vertical layers, with a model top at 0.01 hPa. Predicted distributions of water vapor, ozone, greenhouse gases (CO_2, CH_4, and N_2O) and CFCs (CFC–11 and CFC–12) feedback to the radiative calculations. The present formulation of the GEOS V2 CCM is the same as in Hurwitz et al. [2011b]. The GEOS V2 CCM performed well in the SPARC CCMVal [2010] detailed evaluation of stratospheric processes.

The model's gravity wave parameterization computes the momentum and heat deposition to orographic and non–orographic gravity wave–breaking using the linear saturation theory by Lindzen [1981]. Orographic gravity wave stress is specified using the formulation derived by McFarlane [1987] and given at the top of the subgrid–scale mountains. Subgrid–scale orography is assumed to be horizontally isotropic. Heat transfer due to gravity wave–breaking is computed from the deposition of the gravity wave energy flux into the mean flow following Warner and McIntyre [2001] and Shaw and Shepherd [2009]. In addition, for the conservation of angular momentum and energy, gravity waves stress and energy flux is gradually dissipated in the top five model layers, as suggested by Shaw and Shepherd [2007].

Modeled variability in tropical stratospheric zonal winds depends on the details of the non–orographic gravity wave drag (GWD) scheme. Early versions of the GEOS V2 CCM did not generate a QBO i.e., zonal winds in the equatorial lower stratosphere were generally easterly [see Figures 1b and 2e–h; SPARC CCMVal, 2010]. A new formulation of the non–orographic gravity wave drag scheme allows the model to generate a spontaneous QBO with a realistic period (30 months at 30 hPa and 50 hPa; see Figure 1c) and zonal wind amplitude [see Hurwitz et al., 2011b]. As non–orographic gravity waves often accompany precipitation (e.g., convective and frontal systems; see Richter et al. [2010]), the latitudinal structure of the gravity wave spectrum is designed to mimic the structure of the climatological mean precipitation field. A tropical peak in non–orographic gravity wave stress is necessary for the generation of an internal QBO in the model. A 700–km wavelength is used for the tropical non–orographic waves to prevent an excessive downward propagation of the semi–annual oscillation into the lower stratosphere, and thus contamination of the QBO signal.

Two time–slice simulations will be considered in Section 3 of this paper: One 50–year simulation with an internal QBO (hereafter "QBO") and one 20–year simulation without a QBO ("NQ"). Both simulations are forced by set of SST and sea ice climatologies, each with a repeating annual cycle, with conditions composited from 10 ENSO neutral (NTRL) years that span the satellite era [as in Hurwitz et al., 2011b]. HadISST1 SSTs and sea ice concentrations at 1° x 1° resolution [Rayner et al., 2003] are used to prepare the composites. All simulations used fixed greenhouse gas and ozone–depleting substance boundary conditions representative of the year 2005. Variability related to the solar cycle and volcanic eruptions is not considered.

Modeled temperature, zonal winds and ozone are compared with a composite of 12 observed NTRL years distributed throughout the 1979–2010 period, using the Modern Era Retrospective–Analysis for Research and Applications (MERRA). MERRA is a reanalysis dataset based on an extensive set of satellite observations and on the Goddard Earth Observing System Data Analysis

System, Version 5 (GEOS–5) [Bosilovich et al., 2008; Rienecker et al., 2011]. The MERRA reanalysis has vertical coverage up to 0.1 hPa, and for this study, is interpolated to 1.25° x 1.25° horizontal resolution.

3 Results

3.1 QBO influence on zonal winds and temperature

Seasonal mean zonal wind climatologies in the NQ simulation are shown in Figures 2e–h. Above 100 hPa, tropical zonal winds are easterly throughout the year in this simulation. The tropical zonal wind magnitude maximizes in the upper stratosphere in the DJF and JJA seasons. The stratospheric polar night jets maximize in the winter season, in the respective hemisphere. The modeled winds compare well with the MERRA reanalysis (Figures 2a–d); in NQ, the polar jets are weaker than observed while tropical stratospheric easterlies are stronger than observed (Figures 2e–h).

Inclusion of the modeled QBO makes a significant difference to zonal winds in the stratosphere. Figures 2i–l show zonal wind differences between the QBO and NQ simulations. By definition, in the deep tropics, the modeled QBO increases mean zonal wind magnitudes throughout the year, with the largest increases of 10–20 m s^{-1} in the middle and upper stratosphere. At high latitudes, the sign of the zonal wind differences is generally independent of height: negative differences equatorward of 60° and positive differences poleward of 60° indicate poleward shifting of the polar stratospheric jets. Poleward shifting of the Southern Hemisphere jet is evident throughout the year, while in the Northern Hemisphere it is limited to the transition seasons. During the DJF season, the Arctic jet strengthens by 5 m s^{-1} (in the lower stratosphere) to 15 m s^{-1} (in the upper stratosphere), consistent with the increased frequency of QBO–westerly years in the QBO simulation.

The modeled QBO affects stratospheric zonal wind variability. Zonal wind variability increases significantly in the QBO simulation, as compared with NQ, throughout the tropical stratosphere and in all seasons (Figures 2m–p). The variance of tropical zonal winds increases tenfold in the lower stratosphere, and by 3–5 times in the middle and upper stratosphere. Decreased mid–latitude variability is evident in the DJF and JJA seasons in the SH and in the SON season in the NH.

The GEOS V2 CCM reproduces the Holton–Tan (1980) relation between the phase of the QBO and Arctic vortex strength in winter. In the QBO simulation, 30 hPa zonal winds in the equatorial region are strongly positively correlated with zonal winds in the Arctic stratosphere in November, December and January: the modeled Arctic vortex is relatively weaker during the easterly phase of the QBO (not shown). Furthermore, the modeled QBO enhances polar variability in zonal winds, particularly during the spring and summer seasons. Enhanced variability in the strength of the polar vortices in late winter and spring implies more variability in the timing of the vortex breakup, and thus, more variability in polar ozone. Links between vortex strength and ozone will be discussed further in the next section.

ENSO neutral stratospheric temperatures are well simulated by the model (Figures 3a–h). Consistent with the weaker–than–observed zonal winds (Figures 2a–h), temperatures in the extra–tropical winter stratosphere are biased high in the NQ simulation (i.e., the polar vortices are weaker than in MERRA). The modeled QBO acts to strengthen the polar vortices, cooling the extra–tropical stratosphere in autumn and winter up to 10 K (Figures 3i–l). In addition, decreased temperatures are seen in the Arctic lower stratosphere in boreal spring (Figure 3j). Inclusion of the QBO increases temperatures on the equatorward side of the polar jets, consistent with the poleward shifting of the polar vortices.

QBO–related changes in temperature variability maximize in the middle stratosphere (Figures 3m–p). Tropical variability increases in all seasons. Variability in the polar stratosphere generally increases as a result of the QBO, while there is a region of reduced variability around 60°S, associated with the stronger and more stable Antarctic vortex.

3.2 QBO influence on ozone

Seasonal mean ozone mixing ratio fields, in the NQ simulation, are shown in Figures 4e–h. Ozone maximizes at approximately 10 ppmv in the deep tropics, at 10 hPa, and decreases with latitude. There is little inter–seasonal variability in tropical ozone. Modeled ozone is generally consistent with the MERRA reanalysis, though modeled peak ozone values in the equatorial middle stratosphere are up to 1 ppmv lower than in MERRA (Figures 4a–h). The MERRA ozone product is generally in agreement with MLS v3.3 ozone [Froidevaux et al., 2008; Jiang et al., 2007; Livesey et al., 2008] during the 2005–2010 period, with a slight high bias in the tropical middle stratosphere and low bias in the polar upper stratosphere.

QBO – NQ ozone differences are statistically significant throughout the stratosphere (Figures 4i–l). In all seasons, the peak in ozone mixing ratio around 10 hPa is reduced by ~1 ppmv in the

QBO simulation as compared with NQ. These ozone differences reflect the relative warming of the tropical middle stratosphere in the QBO simulation (see Figures 3i–l and Figure 5). In the Arctic lower stratosphere, inclusion of the QBO reduces ozone in the SON, DJF and MAM seasons; this result is consistent with the relative strengthening of the Arctic vortex and increase in chemical ozone depletion (as discussed in Section 3.1). During the SON or "ozone hole" season, inclusion of the modeled QBO increases ozone mixing ratios (i.e., reduces ozone depletion) in the Antarctic, reflecting increased temperatures in the polar lower stratosphere. In other seasons, the impact of the modeled QBO on Antarctic ozone is not as straightforward: the sign of the mean change in ozone varies as a function of latitude and altitude.

Inclusion of the modeled QBO has a significant impact on ozone variability (Figure 4m–p). Ozone variability increases in the tropics and subtropics in all seasons, and in the Arctic lower stratosphere in DJF, MAM and JJA. Decreased variability is restricted to the uppermost polar stratosphere in spring and summer.

4 Discussion

This paper showed that a model's representation of the QBO makes a significant difference to stratospheric climate and variability. Comparing a GEOS V2 CCM simulation with a realistic, internally generated QBO to one without, the addition of a QBO enhances tropical variability in zonal wind, temperature and ozone throughout the year. Extra–tropical zonal wind variability is also enhanced, mainly in the spring and summer seasons.

Because the QBO is by definition an oscillating phenomenon, one might assume that a modeled QBO does not exert any net impact on stratospheric climate. This work tested and rejected this assumption:

(1) ***Adding an internal QBO signal affects the mean stratospheric climate***.

In the GEOS V2 CCM, inclusion of a QBO signal shifts both polar vortices further poleward. The polar vortices are strengthened, particularly in autumn and winter. The QBO reduces ozone concentrations in the tropical middle stratosphere and Arctic lower stratosphere.

(2) ***The mean response to the QBO depends on the background zonal wind field, in the model version without a QBO signal***.

Because tropical zonal winds in the NQ simulation are generally easterly, there is a relative increase in zonal wind magnitudes in tropical lower and middle stratosphere in the QBO simulation. Extra–tropical differences between the QBO and NQ simulations reflect a bias toward the westerly phase of the QBO: a relative strengthening and poleward shifting the polar stratospheric jets, and a reduction in Arctic lower stratospheric ozone. The annual mean impact of the QBO on the polar stratosphere is larger in the GEOS V2 CCM (up to 12 m s^{-1}, in both hemispheres) than in the MAECHAM4–CHEM CCM (no significant zonal wind differences) [Punge and Giorgetta, 2008], likely reflecting larger QBO – 'no QBO' tropical zonal wind differences in the GEOS V2 CCM and/or increased statistical robustness due to the greater length of the GEOS V2 CCM simulations.

At 10 hPa, equatorial ozone is negatively correlated with temperature (Figure 4). This result suggests that negative QBO – NQ ozone differences (e.g., Figure 4i) in this region can be explained by the relatively higher temperatures in the QBO simulation. Furthermore, the linear relation between ozone and temperature in the tropical middle stratosphere suggests that, in a climate change simulation, inclusion of the QBO would likely affect the modeled representation of observed ozone values but would not affect ozone trends.

Acknowledgements

The authors thank NASA's MAP program for funding, Stacey Frith for processing the model output and Luke Oman for producing the zonal wind frequency spectra and editing the manuscript. MMH is supported by an appointment to the NASA Postdoctoral Program at Goddard Space Flight Center, administered by Oak Ridge Associated Universities through a contract with NASA.

References

Baldwin, M. P., et al. (2001), The quasi–biennial oscillation, Rev. Geophys., 39, 179–229.

Bosilovich, M. (2008), NASA'S modern era retrospective–analysis for research and applications: integrating earth observations, Earthzine, Sep. 26.

Butchart, N., A. A. Scaife, J. Austin, S. H. E. Hare, and J. R. Knight (2003), Quasi–biennial oscillation in ozone in a coupled chemistry–climate model, J. Geophys. Res., 108, D15, doi:10.1029/2002JD003004.

Froidevaux, L., et al. (2008), Validation of Aura Microwave Limb Sounder stratospheric and mesospheric ozone measurements, J. Geophys. Res., 113, D15S20, doi:10.1029/2007JD008771.

Gray, L. J., and J. A. Pyle (1989), A two–dimensional model of the quasi–biennial oscillation of ozone, J. Atm. Sci., 46, 203-220.

Holton, J. R., and H.–C. Tan (1980), The Influence of the equatorial quasi–biennial oscillation on the global circulation at 50 mb, J. Geophys. Res., 37, 2200–2208.

Hurwitz, M. M., P. A. Newman, L. D. Oman, and A. M. Molod (2011a), Response of the Antarctic stratosphere to two types of El Niño events, J. Atm. Sci., 68, 812–822.

Hurwitz, M. M., I.–S. Song, L. D. Oman, P. A. Newman, A. M. Molod, S. M. Frith, and J. E. Nielsen (2011b), Response of the Antarctic stratosphere to warm pool El Niño events in the GEOS CCM, Atmos. Chem. Phys. Discuss., 11, 9743–9767, doi:10.5194/acpd–11–9743–2011.

Jiang, Y. B., et al. (2007), Validation of the Aura Microwave Limb Sounder ozone by ozonesonde and lidar measurements, J. Geophys. Res., 112, D24S34, doi:10.1029/2007JD008776.

Kug, J.–S., F.–F. Jin, and S.–I. An (2009), Two types of El Niño events: cold tongue El Niño and warm pool El Niño, J. Climate, 22, 1499–1515.

Lait, L. R., M. R. Schoeberl, and P. A. Newman (1989), Quasibiennial modulation of the Antarctic ozone depletion, J. Geophys. Res., 94, 11,559–11,571.

Lindzen, R. S. (1981), Turbulence and stress owing to gravity wave and tidal breakdown, J. Geophys. Res., 86, 9707–9714.

Livesey, N. J., et al. (2008), Validation of Aura Microwave Limb Sounder O_3 and CO observations in the upper troposphere and lower stratosphere, J. Geophys. Res., 113, D15S02, doi:10.1029/2007JD008805.

Lu, H., M. P. Baldwin, L. J. Gray, and M. J. Jarvis (2008), Decadal–scale changes in the effect of the QBO on the northern stratospheric polar vortex, J. Geophys. Res., 113, D10114, doi:10.1029/2007JD009647.

McFarlane, N. A. (1987), The effect of orographically excited gravity–wave drag on the circulation of the lower stratosphere and troposphere, J. Atmos. Sci., 44, 1775–1800.

Molod, A. M., L. Takacs, M. Suarez, J. Bacmeister, I.–S. Song, A. Eichmann, and Y. Chang (2011), The GEOS–5 Atmospheric General Circulation Model: mean climate and development from MERRA to Fortuna, Tech. Rep. 104606, V28, Greenbelt, MD, in preparation.

Pawson, S., R. S. Stolarski, A. R. Douglass, P. A. Newman, J .E. Nielsen, S. M. Frith, and M. L. Gupta (2008), Goddard Earth Observing System chemistry–climate model simulations of stratospheric ozone–temperature coupling between 1950 and 2005, J. Geophys. Res., 113, D12103, doi:10.1029/2007JD009511.

Punge, H. J., and M. A. Giorgetta (2008), Net effect of the QBO in a chemistry climate model, Atmos. Chem. Phys., 8, 6505–6525.

Randel, W. J., and J. B. Cobb (1994), Coherent variations of monthly mean total ozone and lower stratospheric temperature, J. Geophys. Res., 99, 5433–5447.

Rayner, N. A., D. E. Parker, E. B. Horton, C. K. Folland, L. V. Alexander, D. P. Rowell, and A. Kaplan (2003), Global analyses of sea surface temperature, sea ice, and night marine air temperature since the late nineteenth century, J. Geophys. Res., 108, D14, 4407.

Richter, J. H., Sassi, F., and Garcia, R. R. (2010), Toward a physically based gravity wave source parameterization in a general circulation model, J. Atmos. Sci., 67, 136–156.

Rienecker, M. M., et al. (2011), MERRA – NASA's Modern–Era Retrospective Analysis for Research and Applications, J. Climate, doi:10.1175/JCLI–D–11–00015.1, in press.

Shaw, T. A., and Shepherd, T. G. (2007), Angular momentum conservation and gravity wave drag parameterization: implications for climate models, J. Atmos. Sci., 64, 190–203.

Shaw, T. A., and Shepherd, T. G. (2009), A theoretical framework for energy and momentum consistency in subgrid–scale parameterization for climate models, J. Atmos. Sci., 66, 3095–3114.

SPARC CCMVal (2010), SPARC Report on the Evaluation of Chemistry–Climate Models, edited by V. Eyring, T. G. Shepherd, and D. W. Waugh, SPARC Report No. 5, WCRP–132, WMO/TDNo. 1526, available at http://www.atmosp.physics.utoronto.ca/SPARC.

Tian, W. S., M. P. Chipperfield, L. J. Gray, and J. M. Zawodny (2006), Quasi–biennial oscillation and tracer distributions in a coupled chemistry–climate model, J. Geophys. Res., 111, D20301, doi:10.1029/2005JD006871.

Warner, C. D., and M. E. McIntyre (2001), An ultrasimple spectral parameterization for nonorographic gravity waves, J. Atmos. Sci., 58, 1837–1857.

Figure Captions

Figure 1: Zonal wind frequency spectra for 4°S–4°N in (a) MERRA, 1979–2009, (b) the NQ simulation, and (c) the QBO simulation.

Figure 2: Seasonal and zonal mean zonal wind, as a function of latitude and altitude, in the NTRL composite in MERRA (a, b, c, d; m s^{-1}) and in the NQ simulation (e, f, g, h; m s^{-1}). (i, j, k, l; m s^{-1}) Seasonal mean zonal wind differences between the QBO and NQ simulations, as a function of latitude and altitude. (m, n, o, p) Ratio of the variance between the QBO and NQ simulations, as a function of latitude, altitude and season. White contours indicate no difference in the mean (variance). Black Xs indicate regions where differences in the mean (variance) are significant at the 95% confidence level.

Figure 3: Seasonal and zonal mean temperature, as a function of latitude and altitude, in the NTRL composite in MERRA (a, b, c, d; K) and in the NQ simulation (e, f, g, h; K). (i, j, k, l; K) Seasonal mean zonal wind differences between the QBO and NQ simulations, as a function of latitude and altitude. (m, n, o, p) Ratio of the variance between the QBO and NQ simulations, as a function of latitude, altitude and season. White contours indicate no difference in the mean (variance). Black Xs indicate regions where differences in the mean (variance) are significant at the 95% confidence level.

Figure 4: Seasonal and zonal mean ozone mixing ratio, as a function of latitude and altitude, in the NTRL composite in MERRA (a, b, c, d; ppmv) and in the NQ simulation (e, f, g, h; ppmv).

(i, j, k, l; ppmv) Seasonal mean zonal wind differences between the QBO and NQ simulations, as a function of latitude and altitude. (m, n, o, p) Ratio of the variance between the QBO and NQ simulations, as a function of latitude, altitude and season. White contours indicate no difference in the mean (variance). Black Xs indicate regions where differences in the mean (variance) are significant at the 95% confidence level.

Figure 5: Temperature versus ozone at 10°S–10°N, 10 hPa in January/February in the QBO simulation (triangles) and NQ simulation (squares). The thick black line denotes the linear fit between temperature and ozone in the QBO simulation.

Figures

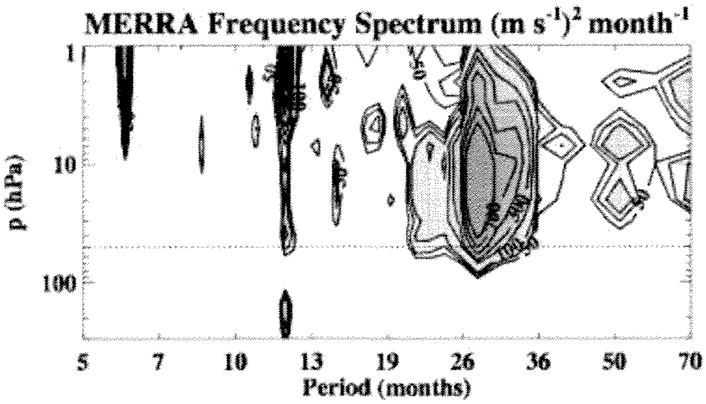

(a)

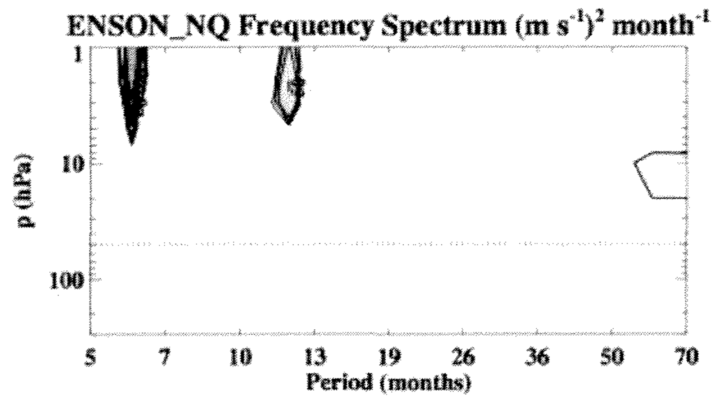

(b)

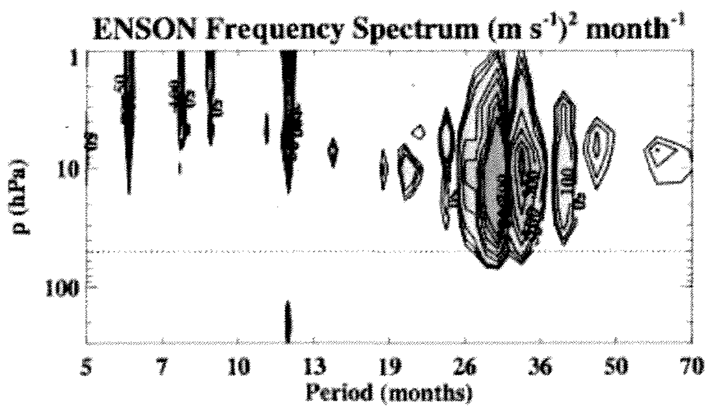

(c)

Figure 1: Zonal wind frequency spectra for 4°S–4°N in (a) MERRA, 1979–2009, (b) the NQ simulation, and (c) the QBO simulation.

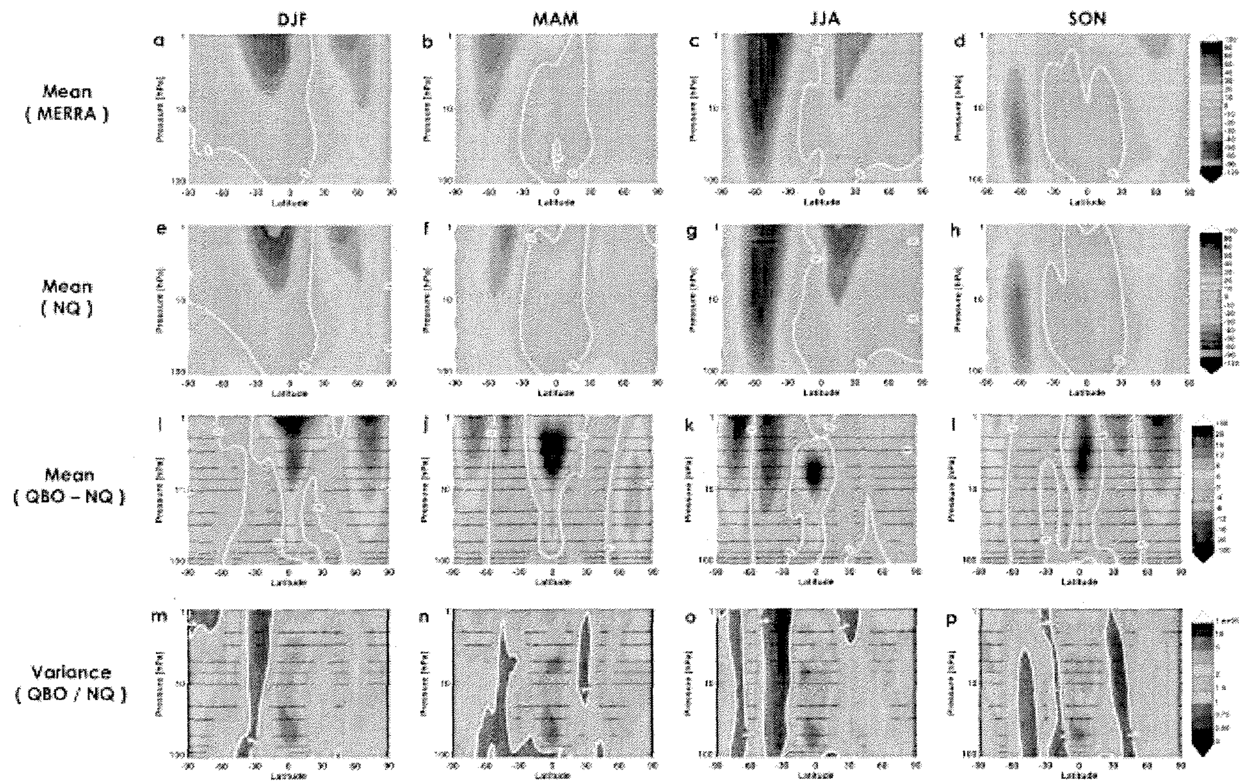

Figure 2: Seasonal and zonal mean zonal wind, as a function of latitude and altitude, in the NTRL composite in MERRA (a, b, c, d; m s^{-1}) and in the NQ simulation (e, f, g, h; m s^{-1}). (i, j, k, l; m s^{-1}) Seasonal mean zonal wind differences between the QBO and NQ simulations, as a function of latitude and altitude. (m, n, o, p) Ratio of the variance between the QBO and NQ simulations, as a function of latitude, altitude and season. White contours indicate no difference in the mean (variance). Black Xs indicate regions where differences in the mean (variance) are significant at the 95% confidence level.

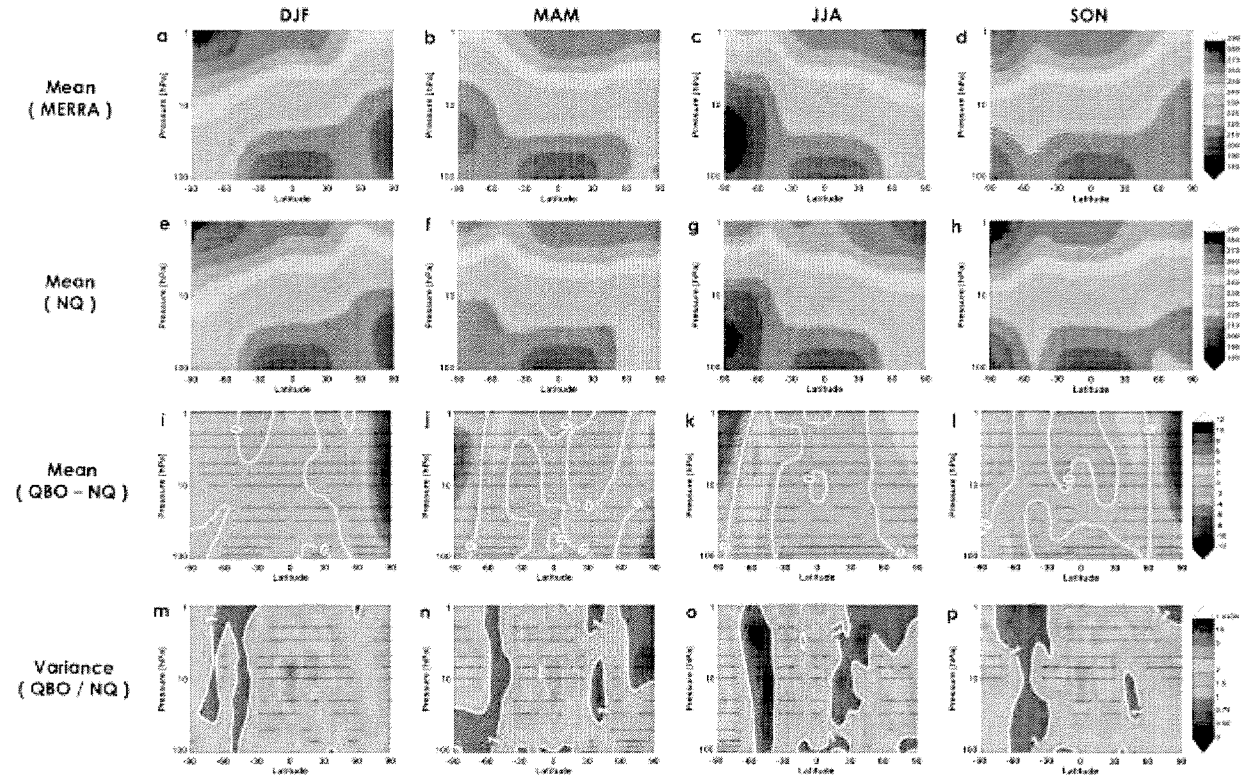

Figure 3: Seasonal and zonal mean temperature, as a function of latitude and altitude, in the NTRL composite in MERRA (a, b, c, d; K) and in the NQ simulation (e, f, g, h; K). (i, j, k, l; K) Seasonal mean zonal wind differences between the QBO and NQ simulations, as a function of latitude and altitude. (m, n, o, p) Ratio of the variance between the QBO and NQ simulations, as a function of latitude, altitude and season. White contours indicate no difference in the mean (variance). Black Xs indicate regions where differences in the mean (variance) are significant at the 95% confidence level.

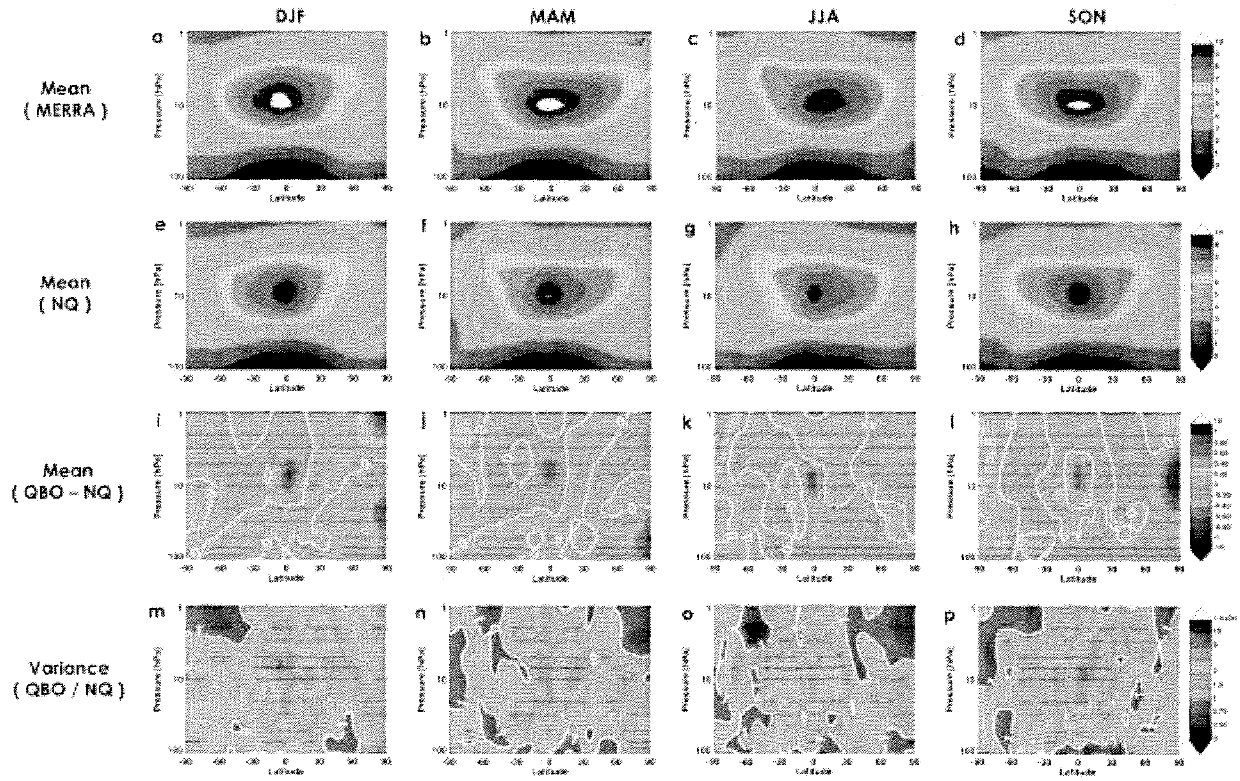

Figure 4: Seasonal and zonal mean ozone mixing ratio, as a function of latitude and altitude, in the NTRL composite in MERRA (a, b, c, d; ppmv) and in the NQ simulation (e, f, g, h; ppmv). (i, j, k, l; ppmv) Seasonal mean zonal wind differences between the QBO and NQ simulations, as a function of latitude and altitude. (m, n, o, p) Ratio of the variance between the QBO and NQ simulations, as a function of latitude, altitude and season. White contours indicate no difference in the mean (variance). Black Xs indicate regions where differences in the mean (variance) are significant at the 95% confidence level.

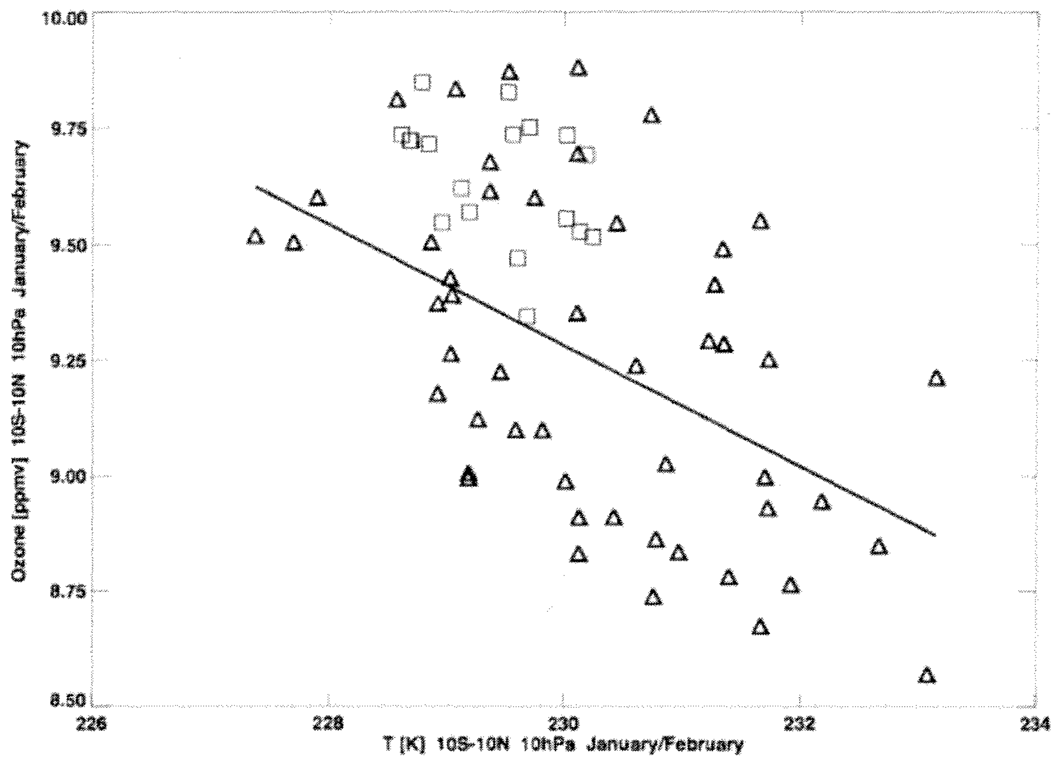

Figure 5: Temperature versus ozone at 10°S–10°N, 10 hPa in January/February in the QBO simulation (triangles) and NQ simulation (squares). The thick black line denotes the linear fit between temperature and ozone in the QBO simulation.